SCIENTIFIC REPORTS

OPEN

Correspondence and
requests for materials
should be addressed to
M.E.B. (mburow@
tulane.edu)

Altered Death Receptor Signaling Promotes Epithelial-to-Mesenchymal Transition and Acquired Chemoresistance

James W. Antoon[1], Rongye Lai[2], Amanda P. Struckhoff[1], Ashley M. Nitschke[3], Steven Elliott[3], Elizabeth C. Martin[3], Lyndsay V. Rhodes[3], Nam Seung Yoon[2], Virgilio A. Salvo[3], Bin Shan[3], Barbara S. Beckman[1], Kenneth P. Nephew[2] & Matthew E. Burow[1,3]

[1]Departments of Pharmacology, Tulane University School of Medicine, Tulane Avenue, New Orleans, LA, USA, [2]Department of Medical Sciences, Indiana University School of Medicine, East 3rd Street, Bloomington, IN, USA, [3]Department of Medicine, Section of Hematology & Medical Oncology, Tulane University School of Medicine, Tulane Avenue, New Orleans, LA, USA.

Altered death receptor signaling and resistance to subsequent apoptosis is an important clinical resistance mechanism. Here, we investigated the role of death receptor resistance in breast cancer progression. Resistance of the estrogen receptor alpha (ER)-positive, chemosensitive MCF7 breast cancer cell line to tumor necrosis factor (TNF) was associated with loss of ER expression and a multi-drug resistant phenotype. Changes in three major pathways were involved in this transition to a multidrug resistance phenotype: ER, Death Receptor and epithelial to mesenchymal transition (EMT). Resistant cells exhibited altered ER signaling, resulting in decreased ER target gene expression. The death receptor pathway was significantly altered, blocking extrinsic apoptosis and increasing NF-kappaB survival signaling. TNF resistance promoted EMT changes, resulting in a more aggressive phenotype. This first report identifying specific mechanisms underlying acquired resistance to TNF could lead to a better understanding of the progression of breast cancer in response to chemotherapy treatment.

B reast is the leading site of new cancers in women, with approximately 230,480 new cases diagnosed in 2011[1]. Treatment for breast cancer varies depending on tumor stage and molecular characteristics. Unfortunately, for those receiving chemotherapy only 50–70% respond to first line treatment[2]. The response rate decreases steadily with subsequent therapy, with 20–30% and 10% responding to second and third line treatments, respectively[2]. Almost all chemotherapeutic agents used in the treatment of breast cancer develop resistance mechanisms that are responsible for recurrence. A number of mutations and cellular mechanisms are associated with resistance to chemotherapy-induced cell death, many of which are found upstream or downstream of the initiation of apoptosis[3]. While several chemoresistance mechanisms are known, the ability of a cell to transition to a chemoresistant state in response to therapy is poorly understood.

The death receptor signaling pathway is a primary mediator of cell fate[4]. The cytokine, TNF, is responsible for activating both apoptotic and survival pathways. The mechanisms through which these death and survival signals interact to determine cell fate remains unclear. TNF has two extracellular receptors, TNFR1 (p55) and TNFR2 (p75) and TNFR1 is primarily responsible for regulating the apoptotic activity of TNF[5]. However, binding of TNF to TNFR1 alone is not sufficient to induce apoptosis[5,6]. A number of downstream signaling cascades determine the sensitivity of the cell to TNF- induced cell death. Binding of TNFR1 to its ligand results in recruitment of various proteins to the intracellular ''death domain'' portion of the receptor[6]. The formation of this TNFR1 complex leads to activation of a number of downstream signaling pathways, such as nuclear factor kappa B (NF-κB)[7]. These pathways transmit either the apoptotic, such as sphingomyelinase, or survival signals, such as NF-κB, or NFR[8].

While the ability of tumor cells to evade extrinsic cell death is well documented, how tumor cells alter the death receptor cascade to promote survival rather than induce apoptosis is not well understood[9,10]. Direct mutations limiting the effect of death receptor signaling present in drug resistant tumors correlate with a worse clinical
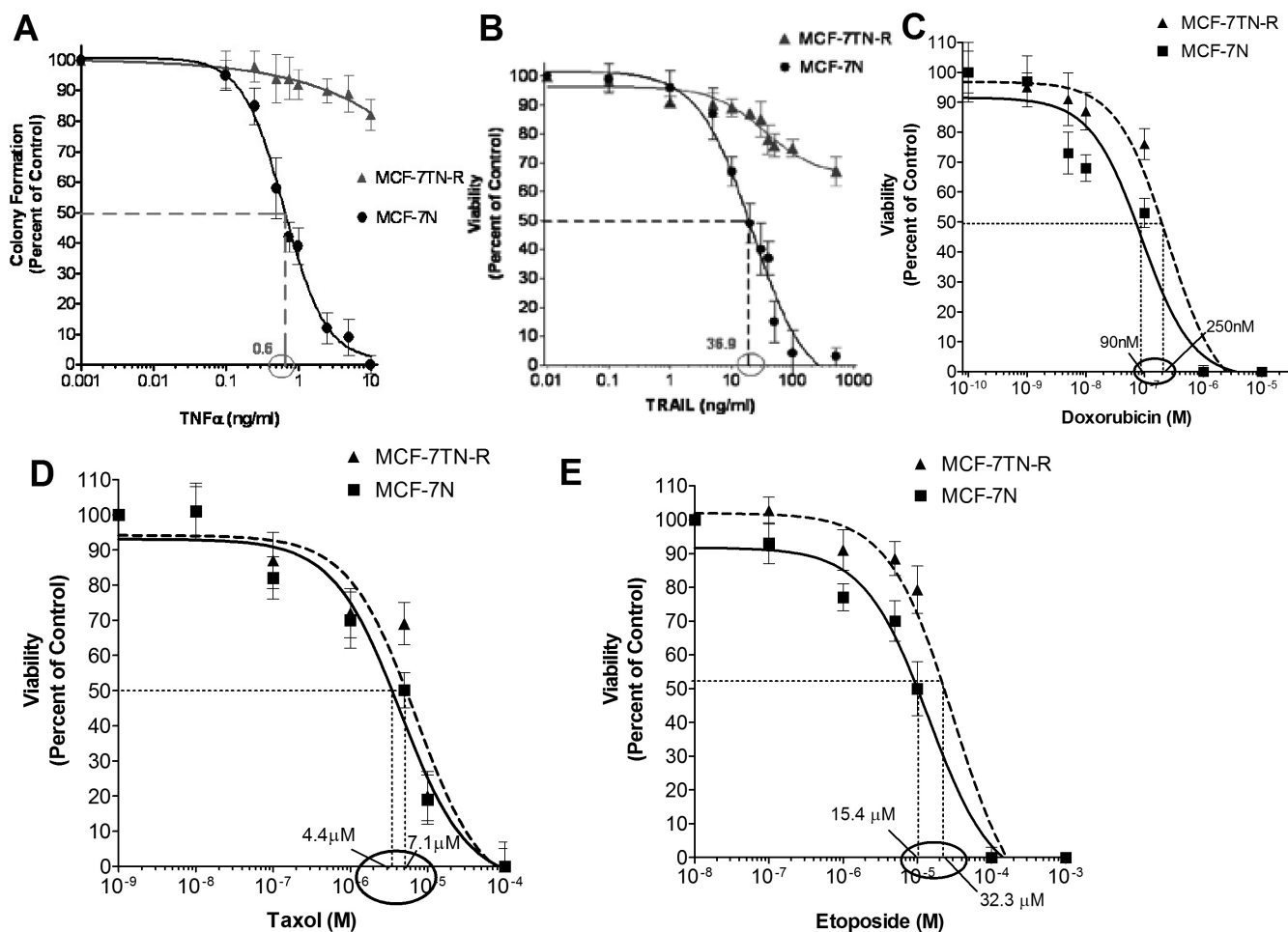
Figure 1 | The MCF-7TN-R breast cancer cell variant exhibits increased resistance to clinical chemotherapeutics. (A) MCF-7N and MCF-7TN-R cells were plated at 500 cells per 60 mm². The following day, cells were treated with varying concentrations of TNF for 24 hrs and then cultured for 10-14 days. Data are presented as percent of vehicle treated samples. Mean values ± S.E.M. of 3 independent experiments in duplicate are reported. (B) Cultured MCF-7TN-R or MCF-7N breast cancer cell variants were treated with increasing doses of TRAIL, (C) doxorubicin, (D) taxol or (E) etoposide. After 48 h, cell viability was estimated using the MTT assay. Data are presented as percentage of viability of vehicle-treated control cells. Mean values ± S.E.M. of four independent experiments in triplicate are reported.

outcome. For example, high expression levels of TNF correlate with a favorable prognosis while metastatic breast cancer tumors with poor prognosis exhibit decreased endogenous levels of TNF or mutated TNF promoter regions[11,12]. Furthermore, exogenous administration of death receptor ligands can overcome this endogenous drug resistance[13]. Several downstream effectors of TNF are also known to be involved in drug resistance. Resistant cells can alter the downstream cellular machinery involved in apoptosis to counteract the end product of death receptor induced cell death[14]. Increased expression of the anti-apoptotic Bcl-2 family members, Bcl-2 and Bcl-xL, and decreased expression of pro-apoptotic members, Bax and Bid, are common resistance mechanisms aimed at disrupting mitochondrially initiated apoptosis[15,16]. Changes in the NF-κB signaling cascade downstream of TNF promote resistance in breast cancer cells by increasing expression of inhibitor of apoptosis proteins (IAPs), FLICE-inhibitory protein (FLIP), Bcl-xL and cyclin D[17]. Increased NF-κB signaling also promotes the epithelial-to-mesenchymal transition (EMT) and cross-talk with the estrogen receptor-α (ER) to promote hormone-independent growth and metastasis[3,18].

We previously generated a cellular model for the transition of breast cancer from an ER-positive, endocrine and chemosensitive state to a multidrug resistant phenotype[19]. TNF resistance was generated by prolonged and progressive exposure of MCF-7 cells to TNF to produce the isogenic MCF-7TN-R cell system. These MCF-7TN-R

cells exhibited complete resistance to TNF-induced cell death, with exposure to TNF resulting in increased phosphorylated, but not total levels of downstream NF-κB signaling[20–22]. We have previously demonstrated that these cells do not generate intracellular ceramide, a well known marker of chemoresistance in response to chemotherapeutic treatment[19,23,24].

In this study, we investigated the molecular and genetic alterations involved in TNF-induced chemoresistance. We identified and characterized three major pathways involved in this acquired chemoresistance model: ER, Death Receptor, and EMT, and examined specific protein and gene expression alterations involved in these key pathway that may promote chemoresistance. Our results suggest that these pathways play a role in transition of chemosensitive to chemoresistant cells and may represent targets for new therapies to overcome breast cancer drug resistance.

Results

TNF resistance promotes multidrug resistance and enhanced tumorigenesis. Our laboratory has previously demonstrated that the MCF-7TN-R cell system is resistant to both short-term TNF-induced ceramide generation and cell death[19,25]. To confirm the TNF resistance, we examined whether these cells were resistant to the cytotoxic effects of TNF in long-term assays. As seen in Figure 1a, MCF-7 cells exhibited a dose-dependent decrease in clonogenic
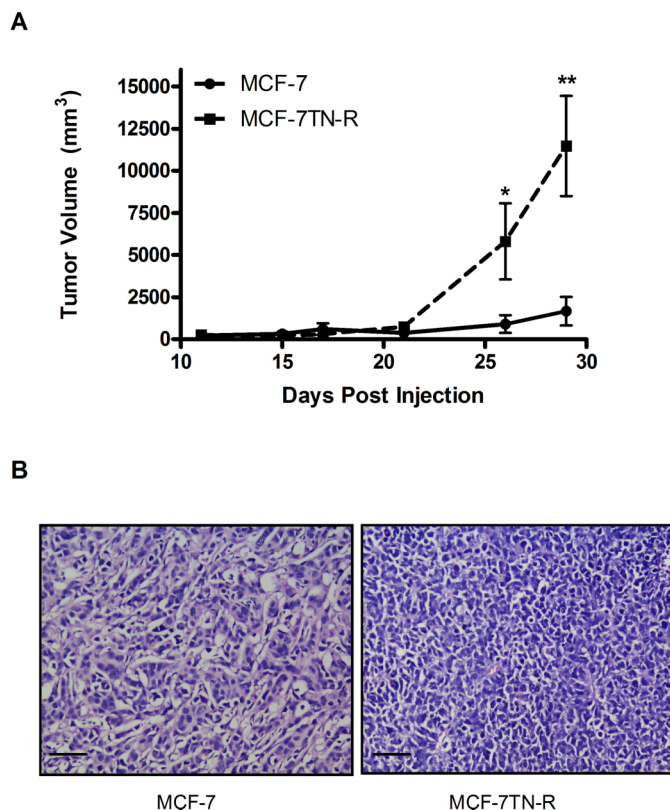
Figure 2 | **TNF resistance promotes hormone dependent and hormone independent tumor growth.** (A) MCF-7 and MCF-7TN-R cells were injected in the mammary fat pads of female ovariectomized mice with exogenous E2 pellets. Tumor volume was measured every 2 d. (B) Representative H&E staining images (100x) from MCF-7 and MCF-7TN-R endpoint tumors. Scale bar equal to 500 μm.

survival in response to prolonged TNF treatment. The IC_{50} of TNFα for colony formation of the MCF-7N cells was 0.64 ng/ml, while the MCF-7TN-R variant showed no significant decrease in colony number eight days after a 24 hr exposure to TNFα, suggesting complete functional resistance to TNF.

To determine whether resistance in the MCF-7TN-R cells was restricted to TNFα, or if it was a more general mechanism of chemoresistance, effects of established cytotoxic and chemotherapeutic agents were investigated. Treatment with TNFα-related apoptosis-inducing ligand (TRAIL) resulted in a concentration-dependent decrease in MCF-7 cell viability as measured by MTT with an IC_{50} of 36.9 ng/ml (Figure 1b). Although the MCF-7TN-R variant was more sensitive to the cytotoxic effects of TRAIL compared to TNFα, the MCF-7TN-R variant was resistant to the growth inhibitory effects of TRAIL vs. the MCF-7 cell variant. The highest concentration of TRAIL tested (100 ng/ml) decreased MCF-7 viability by 100%, while the same concentration decreased MCF-7TN-R viability by only 36.3 ± 7.2 % (p<0.001).

We next investigated whether TNF conferred resistance to the clinical chemotherapeutics, doxorubicin, taxol and etoposide. Though not completely resistant to these clinical agents, there was a nearly two-fold increase in IC_{50} values compared to parental MCF-7 cells (Figure1c-e). The MCF-7TN-R cells were more resistant to doxorubicin with an IC_{50} of 0.26 μM compared to 0.09 μM (p<0.01) for MCF-7 cells. Similar results were found for etoposide (IC_{50} 15.4 μM versus 32.3 μM for MCF-7 and MCF-7TN-R respectively, (p < 0.05), and taxol (IC_{50} 4.4 μM versus 7.1 μM (p<0.001) for MCF-7 and MCF-7TN-R, respectively). Taken together, these results suggest that MCF-7TN-R cells represent a model of transition to a multidrug resistant phenotype in human breast cancer cells.
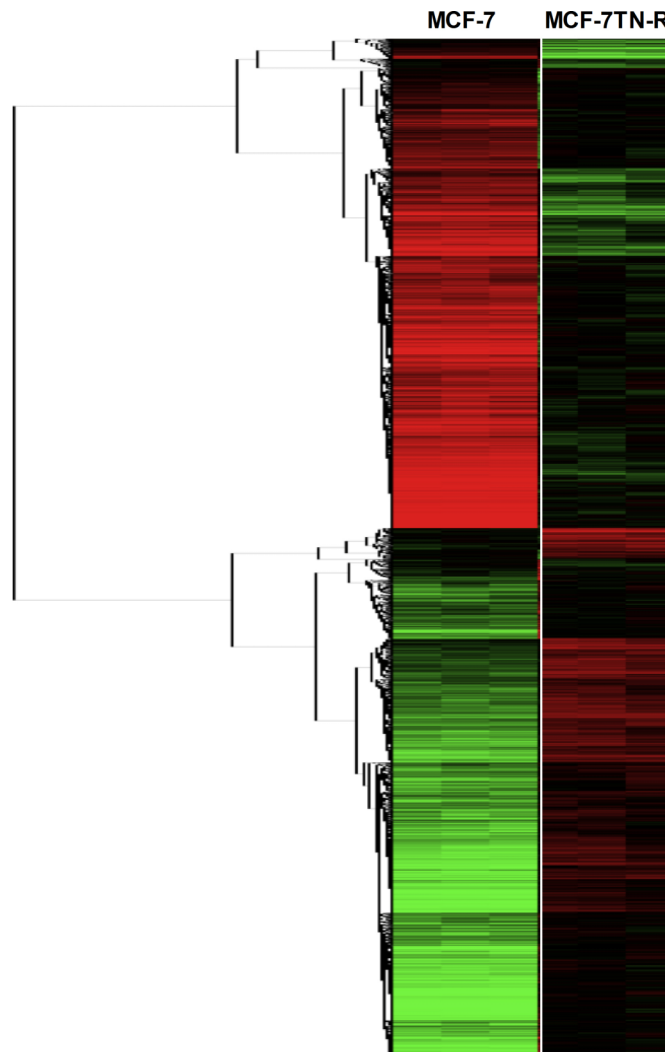

Figure 3 | **Clustering analysis of mRNA expression profiles of MCF-7 and MCF-7TN-R cells.** MCF-7 (left column) and MCF-7TN-R (right column) have distinctive gene expression patterns, with samples of same cell lines clustered together. Trees on the left are gene clusters. Red color indicates up-regulation, and green color indicates down-regulation.

Given the increased proliferative rates of clinical chemoresistant tumors, we examined growth of the TNF resistant cells as xenograft tumors in nude mice. As seen in Figure 2a, at 29 days post-injection there was a 5-fold increase p-value in MCF-7TN-R tumor volume compared to parental MCF-7 cells. Furthermore, endpoint tumor analysis revealed increased cellularity in the MCF-7TN-R compared to MCF-7 tumors (Figure 2b). These results demonstrate MCF-7TN-R cells exhibited an increased tumorigenic phenotype in addition to multidrug resistance.

Global gene expression profiles associated with TNF resistance. In order to determine the mechanisms involved in enhanced TNF-mediated tumorigenesis, global gene expression profiling was performed on MCF-7TN-R cells and compared to MCF-7-VEC cells. Unsupervised hierarchical clustering was performed on the mRNA profiles to further investigate genome-wide transcriptional patterns. Expression data was log-transformed and median-centered between arrays and within genes. Visualization of clustering results showed that samples of the same cell types clustered together, validating that MCF-7TN-R are distinctive from parental MCF-7 cells on a molecular level (Figure 3). The analysis identified 3404 significantly altered genes: 1636 upregulated and 1357 downregulated transcripts

Table 1 | Cancer Signaling Pathway Gene Expression Changes

Pathway Name	Impact Factor	Number of Genes in Pathway	Genes Altered	Percent Pathway Altered	p-value
Axon Guidance	25.26	129	43	33.33	5.87E-10
Tight Junction	15.01	135	36	26.67	6.54E-06
MAPK Signaling	13.67	272	60	22.06	7.18E-06
Pathways in Cancer	13.18	330	69	20.91	1.08E-05
Regulation of Actin Cytoskeleton	12.86	217	50	23.04	1.17E-05
Focal Adhesion	12.71	203	47	23.15	1.84E-05
Adherens Junction	43.81	78	23	29.49	5.41E-05
Small Cell Lung Cancer	10.86	86	24	27.91	9.93E-05
Adipocytokine Signaling	10.97	67	20	29.85	1.35E-04
p53 Signaling Pathway	9.00	69	19	27.54	6.10E-04
Chronic Myeloid Leukemia	9.16	75	20	26.67	6.96E-04
Cell Adhesion Molecules (CAMs)	220.47	134	30	22.39	9.98E-04
Apoptosis	8.43	89	22	24.72	1.17E-03
ECM-Receptor Interaction	8.61	84	21	25.00	1.28E-03
ABC Transporters	7.24	44	13	29.55	2.15E-03
Pancreatic Cancer	8.17	72	18	25.00	2.76E-03
Fc epsilon RI Signaling	7.31	78	19	24.36	2.94E-03
Colorectal Cancer	8.11	84	20	23.81	3.08E-03
Non-small Cell Lung Cancer	7.41	54	14	25.93	5.53E-03
Leukocyte Transendothelial Migration	313.99	119	25	21.01	6.05E-03
Prostate Cancer	7.01	90	20	22.22	7.02E-03
Cell Cycle	5.60	118	24	20.34	1.17E-02
Bladder Cancer	7.46	42	11	26.19	1.22E-02
Glioma	6.98	65	15	23.08	1.28E-02
Melanoma	8.02	71	16	22.54	1.30E-02
Epithelial Cell Signaling in H. Pylori Infection	5.20	68	15	22.06	1.92E-02
TGF-beta Signaling	7.87	87	18	20.69	2.08E-02
Phosphatidylinositol Signaling	11.31	76	16	21.05	2.43E-02
PPAR Signaling	4.52	70	15	21.43	2.46E-02
B cell Receptor Signaling	5.94	65	14	21.54	2.81E-02
Acute Myeloid Leukemia	6.45	59	13	22.03	2.83E-02
Systemic Lupus Erythematosus	4.41	144	26	18.06	3.39E-02
VEGF Signaling	5.63	74	15	20.27	3.88E-02
ErbB Signaling	10.20	87	17	19.54	4.00E-02
Hedgehog Signaling	3.57	57	12	21.05	4.69E-02

(Fig 3). Although the altered genetic profile was diverse, it could be organized into functional signalling categories using the Kyoto Encyclopedia of Genes and Genomes database and Gene Ontology algorithms (Table 1).

Altered death receptor pathway enhances NF-κB survival signaling. Given the multidrug resistant nature of these cells, we next examined the death receptor pathway changes that resulted in TNF and clinical chemotherapeutic resistance using pathway analysis of microarray data for genomic death receptor pathway alterations. There were numerous changes in the TNF pathway; however, there was an overall decrease in expression of genes responsible for programmed cell death (Supplemental Table 1), including down-regulation of death receptors, scaffolding proteins and downstream caspases. Notably, decreased TNFR1 expression and TRAD expression was observed, but there was no change in TNFR2 or TRAF expression. Further analyses of transcription factors regulating TNF and TRAD revealed multiple expression changes. Specifically, 17 out of the 45 (38%) TRADD transcription factors were significantly altered in MCF-7TN-R cells compared to MCF-7 (Supplemental Table 2). Similarly, 51 out of the 112 (46%) TNFR1A transcription factors were significantly altered in MCF-7TN-R (Supplemental Table 3). To further validate the above genomic findings, we determined protein expression levels of both TNF receptors, TNFR1 and TNFR2. As seen in Figure 4a, cellular protein levels of TNFR1 were markedly decreased with a concomitant increase in TNFR2 compared to MCF-7 cells. Densitometric analysis was performed and confirmed these protein findings (Supplemental Table 4). These results correlated with

the gene expression alterations described above. The differential expression of death receptor pathway transcription factors likely contributed to the TNF resistance in these MCF-7TN-R cells.

In order to better understand the impact of death receptor changes, microarray results were analyzed for alterations in NF-κB protein expression and NF-κB mediated gene expression. Altered expression of several NF-κB target genes was observed, including increased BIRC2 (IAP1), correlating with protein and transcriptional activity changes noted above (Supplemental File 5). Interestingly, p65 regulated ZEB1 and ZEB2 were increased (p<0.001) 12.3- and 8.7-fold, respectively. ZEB1 is known to repress E-cadherin and miRNAs involved in EMT and overexpression of both ZEB1 and ZEB2 are characteristic markers of EMT changes[26].

Given the enhanced NF-κB- mediated gene expression, we hypothesized that the increased survival seen in these cells resulted from increased NF-κB signaling to overcome TNF- mediated cell death. The NF-κB transcription factor consists of five subunits, with the p50 and p65 subunits believed to be involved breast cancer promotion and progression[27]. Microarray results for the intracellular NF-κB subunits were further validated at the protein levels. As seen in Figure 4a, MCF-7TN-R cells exhibit increased protein expression levels of the p50 subunit, but not the p65 subunit of NF-κB. There was also a decrease in the expression of the inhibitory IκB protein in resistant MCF-7TNR compared to parental sensitive MCF-7 cells (Figure 4a, Supplemental Table 4). These NF-κB protein alterations likely resulted in the enhanced NF-κB survival signaling in these cells.

Given the importance of p65 in the pathologic growth of breast cancer, we next determined whether the activity of p65 in MCF-7TN-R
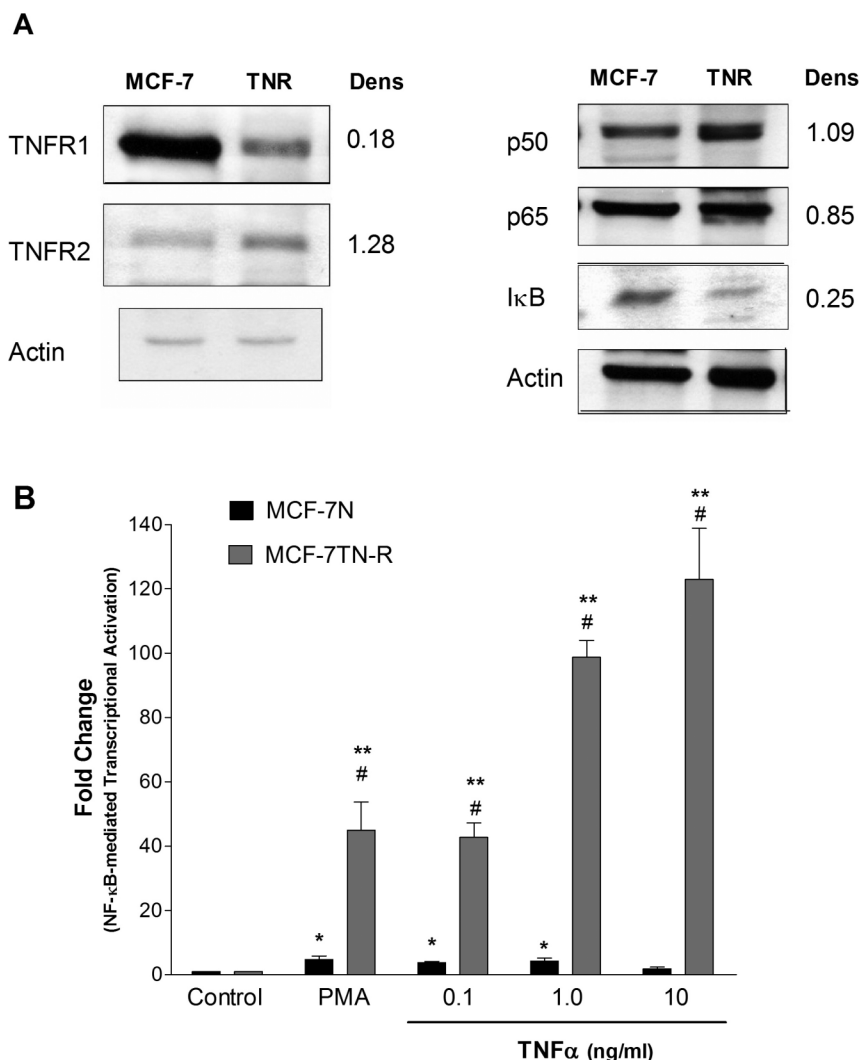
Figure 4 | Resistant MCF-7TN-R cells exhibit increased NF-κB signaling. (A) MCF-7 or MCF-7TN-R cells were plated at 1.5x10⁶. Twenty-four hours later the cells were harvested, lysed and immunoblotting used to determine the relative expression of TNFR1, TNFR2, p50, p65 or IκB. (B) MCF-7 and MCF-7TN-R cells were transiently transfected with pFC-NF-κB-luciferase plasmid. Following transfection, cells were treated with vehicle, PMA (positive control) or indicated concentrations of TNF. Cells treated with vehicle were set to 1. Data points and error bars represent the mean ± S.E.M. of three independent experiments in duplicate (*** $p < 0.001$, ** $p < 0.01$, *$p < 0.05$).

was altered compared to MCF-7 cells[18,28,29]. A p65 luciferase plasmid was transiently transfected into both lines, and p65 transcriptional activity measured after TNF treatment. MCF-7TN-R cells exhibited markedly increased p65 transcription activity in response to TNF treatment compared to MCF-7 cells (Figure 4b). In MCF-7TN-R cells, treatment with TNFα resulted in a dose-dependent increase in NF-κB transcriptional activity. The level of induction of NF-κB was greater in the MCF-7TN-R variant than the MCF-7N at all doses tested (42.8 ± 4.5 versus 3.7 ± 0.4, 98.9 ± 5.2 versus 4.3 ± 0.9 fold, and 122.9 ± 15.9 versus 2.4 ± 0.5 ($p < 0.05$) for 0.1, 1.0, and 10 ng/ml TNFα, respectively). In addition, MCF-7TN-R cells demonstrated a greater activation of NF-κB following stimulation with PMA than MCF-7 cells (44.2 ± 5.9 versus 3.8 ± 0.7, respectively)($p < 0.05$). The greater activation of the NF-κB pathway in the resistant cell line as compared to the sensitive parental line suggests a role for NF-κB in the increased survival of these cells. Taken together, these results demonstrate the specific death receptor pathway alteration involved in acquired breast cancer chemoresistance.

TNF resistance confers an EMT phenotype to previously sensitive breast cancer cells. As mentioned above, the ZEB1 and ZEB2 EMT transcription factors were differentially expressed in MCF-7TN-R

cells compared to MCF-7 cells. EMT changes are known to promote migration and metastasis in breast cancer. We next analyzed the above microarray data for differences in the expression levels of 168 genes known to promote EMT in breast cancer. The results were similar to the clustering result using the whole mRNA profiles (Supplemental Figure 1). The EMT gene expression profile was markedly altered in MCF-7TN-R compared to MCF-7 cells, suggesting the phenotypic appearance of MCF-7TN-R cell is a result of progressive EMT changes (Supplemental Table 6).

MCF-7TN-R cells are phenotypically distinct from MCF-7 cells, and appear more similar to a basal-like cancer than their luminal parental cells (Figure 5a). In order to validate the above gene expression findings, immunofluorescence was performed using E-cadherin, an epithelial cell marker, and vimentin, a mesenchymal cell marker. The MDA-MB-231 cell line, a well-studied metastatic, EMT model, was utilized as a positive EMT control. Loss of E-cadherin and increased vimentin staining were observed, consistent with EMT changes in MCF-7TN-R cells compared to MCF-7 controls (Figure 5b). Expression levels of both of these proteins were similar to the MDA-MB-231 cell line.

To further validate the EMT-like phenotype, RT-PCR analysis was performed for Twist, Snail and Slug, known EMT promoting
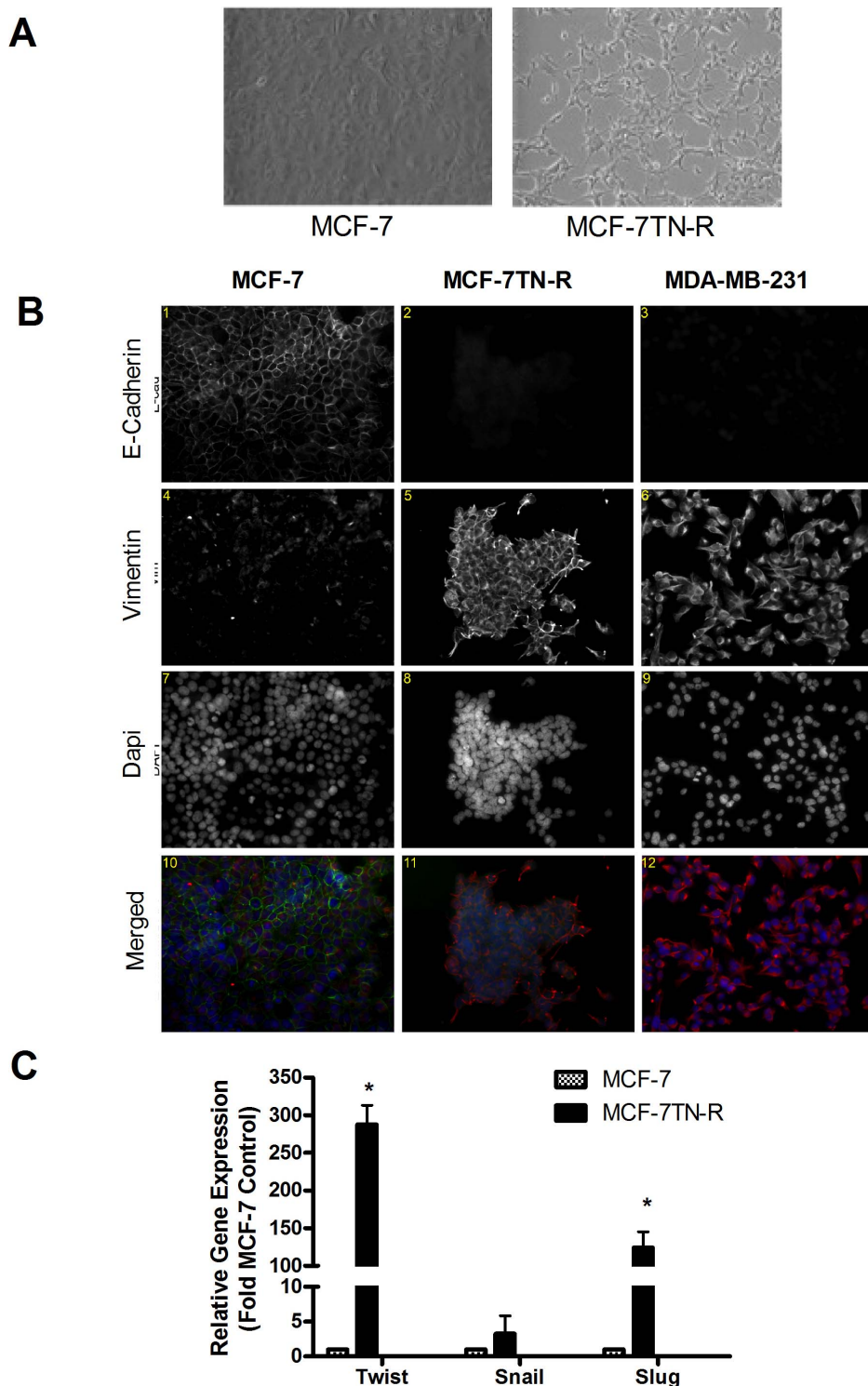
Figure 5 | Increased markers of EMT in resistant MCF-7TN-R cells. (A) MCF-7, MCF-7TN-R, and MDA-MB-231 cells were cultured in eight-well chamber slide for 48 hours. Indirect immunofluorescence was carried out to examine the expression of e-cadherin and vimentin, as described in the Materials and methods section. The nucleus was counter-stained with DAPI. Pseudocolors were assigned as follows: red, E-cadherin; green, vimentin; and blue, nucleus. (B) mRNA gene expression of the EMT markers Twist, Snail and Slug were quantified using qPCR in MCF-7 and MCF-7TN-R cells. Mean values ± SEM of three independent experiments in triplicate are reported.

genes[26,30–32]. Twist, Snail and Slug are known to repress E-cadherin expression in breast cancer[26,32]. Expression of both Twist and Slug was markedly increased in MCF-7TN-R cells compared to MCF-7 cells, with mRNA levels of 287.70 fold ± 25.26 (p<0.01) and 124.30 fold ± 21.01 (p<0.05), respectively (Figure 5c). Snail expression also trended up but did not reach statistical significance. Taken together,

these results are consistent with an EMT phenotype in our TNF resistant cell model.

Estrogen receptor pathway alterations in chemoresistant breast cancer. EMT is associated with the loss of ER expression and hormone independent growth[33]. Studies have shown also shown
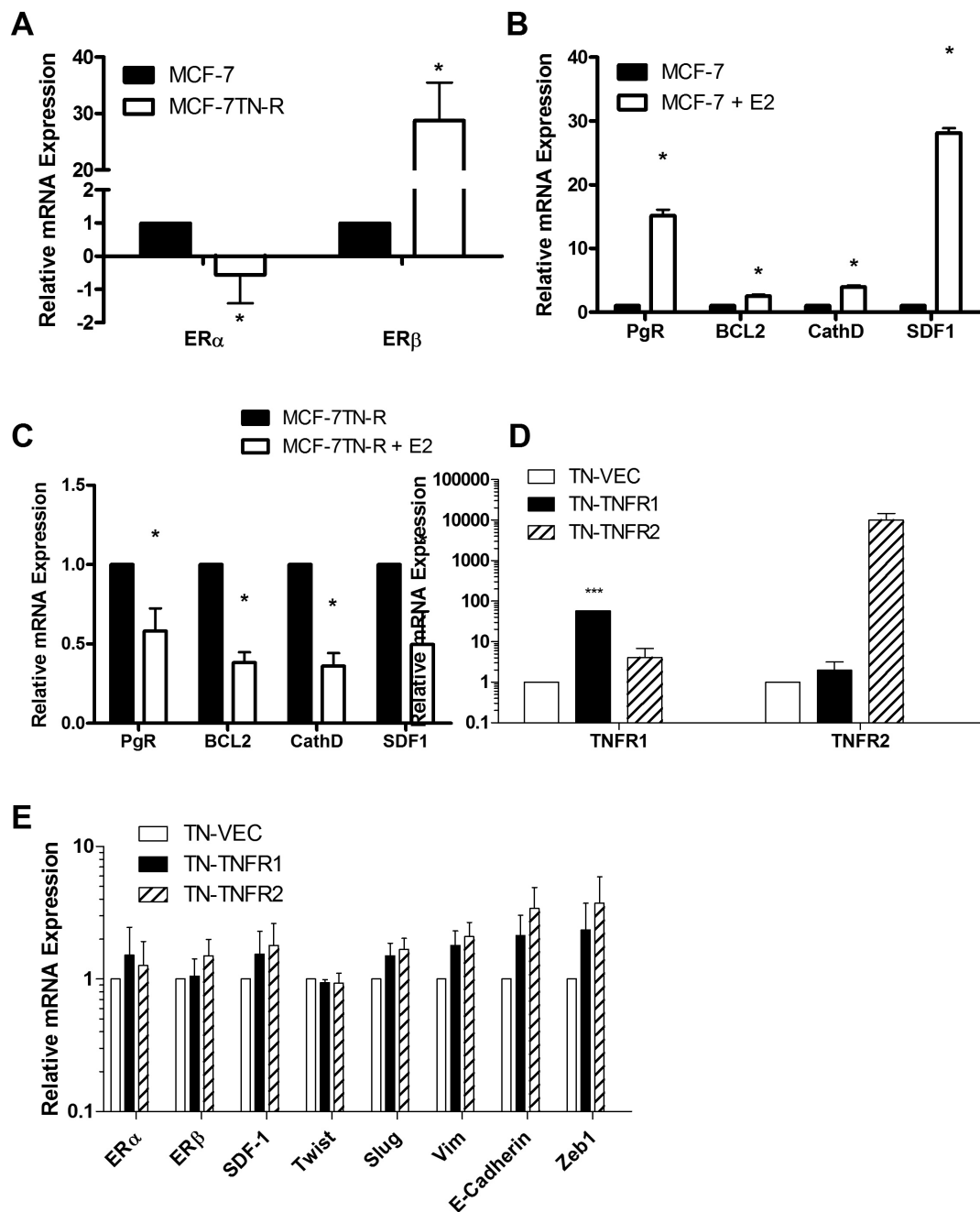
Figure 6 | Decreased ER signaling in MCF-7TN-R cells. (A) Basal mRNA expression levels of ERα and ERβ in MCF-7 and MCF-7TN-R cells were quantified using qRT-PCR. Mean values ± SEM of three independent experiments in triplicate are reported. (B) mRNA expression levels of the ER-mediated genes PgR, BCL-2, Cathepsin D and SDF-1 were quantified using qPCR. mRNA expression was determined in MCF-7 (left) and MCF-7TN-R (right) cells both in the presence and absence of estrogen. Data points and error bars represent the mean ± S.E.M. of three independent experiments in duplicate (*** p < 0.001, ** p < 0.01, *p < 0.05).

cross-talk between TNF-induced survival signaling and both estrogen-mediated and hormone independent tumor proliferation[34,35]. Given the enhanced EMT changes in MCF-7TN-R, we next determined whether the ER pathway was involved in their increased tumorigenesis. To investigate ER genomic activity, clustering analysis was performed on 51 known ER-mediated genes. Results of this analysis were similar to clustering using the whole mRNA profiles (Supplemental Figure 2) and there was marked downregulation of ER-regulated gene expression (Supplemental Table 7). The loss of ER function was confirmed using qPCR analysis of ER gene expression. As seen in Figure 6a, TNF resistance resulted in a loss of ER mRNA expression compared to parental cells. The decreased ER mRNA in

these cells resulted in diminished downstream ER-mediated gene expression (Figure 6b,c).

Given the significant decrease of TNFR1 expression observed (Figure 4a), it was of interest to further evaluate the role of this receptor in in this model system for death receptor resistance. Transient expression of TNFR1 and TNFR2 in our MCF-7TN-R cell system (TN-TNFR1 and TN-TNFR2, respectively) resulted in strong expression of TNFR1 and weak expression of TNFR2 in TN-TNFR1 and TN-TNFR2 cells, respectively (Figure 6d). We then performed qRT-PCR for critical genes involved in death receptor, EMT and ERα signaling and compared results to parental MCF-7TN-R cells and sensitive MCF-7 cells. As seen in Fig 6e, forced overexpression of

TNFR1 did not significantly alter the genetic ERα and EMT changes found in the resistant cell line. We further generated stable MCF-7TN-R cells overexpressing TNFR1 and TNFR2, which provided similar results to the transient model system (data not shown).

Discussion

Chemoresistance is a primary cause of clinical breast cancer treatment failure. Yet, our understanding of the mechanisms involved in the progression of breast cancer to a drug resistant phenotype remains limited. Development of resistance to cytokines such as TNF, may be crucial to the development of primary tumors *in vivo*[36]. Exposure to these endogenous death receptor ligands during early stages of tumor development or during chemotherapeutic treatment may select for an apoptotically resistant population of neoplastic cells. Therefore, development of resistance to TNF may select for breast tumors with an anti-apoptosis and multi-drug resistant phenotype.

In order to identify and study signaling pathways involved in chemoresistance, TNF-resistant MCF-7TN-R cells were derived from TNF-sensitive MCF-7 cells[37]. We demonstrate here that TNF-resistance also confers resistance to the clinical chemotherapeutic agents TRAIL, etoposide, paclitaxel and doxorubicin. These resistant cells exhibited increased tumorigenesis and tumor growth. While TNF and the ER exert opposing effects on ER-positive breast cells, interaction between these pathways has recently been elucidated. Lee *et al* found that treatment of MCF-7 cells with TNF resulted in decreased ER protein and mRNA expression[38]. This ER knockdown was partially reversed with pharmacological inhibition of Akt, suggesting that the PI3K/Akt pathway is involved in the interaction between these two pathways[39]. Additionally, treatment with TNF induced upregulation of NF-κB- mediated gene transcription. Others have shown that increased NF-κB activity in response to TNF results in transition to a basal-like phenotype with loss of ER expression[40]. Furthermore, studies have shown that increased ER expression decreases NF-κB affinity for DNA binding. Conversely, increased expression of NF-κB results in decreased expression of ER regulated proteins[41]. This may be through regulation of the toll-like receptor TLR, which negatively regulates ER expression via NF-κB gene regulation[42]. TNF induced NF-κB transcription is also known to cross-talk with the EGFR pathway to promote hormone independent growth[43]. We also note increased expression of Twist, which has been shown to decrease ER expression and promote hormone independence[44]. Therefore, our findings that prolonged exposure to TNF results in the loss of estrogen expression and altered NF-κB is consistent with previously published results.

We report here several potential mechanisms for acquired apoptotic resistance in the death receptor signaling pathway. Resistant cells exhibited increased protein expression of p75 TNFR2 and decreased protein expression of p55 TNFR1, which promotes the apoptosis signal of TNF. The increased TNFR in MCF-7TN-R protein levels, despite similar mRNA expression levels in resistant- vs. sensitive-cells, could be due to increased protein stabilization, altered microRNA expression and decreased TNFR1 protein degradation in MCF-7TN-R cells. These death receptor changes are consistent with previously published studies in TNF-resistant MCF-7 variants[45]. Evidence to support our findings of decreased TNFR1 in our TNF resistant model can be found in several recent studies. Zyad *et al* demonstrated an association between TNFα resistance and decreased TNFR1 expression, and Sprowl *et al* show that both paclitaxel resistant breast cancer and doxorubicin resistant breast cancer exhibit decreased TNFR1 and increased TNFR2 signaling[9,46,47]. These results correlate well with our data demonstrating that TNFR1 and TNFR2 alterations are associated with increased resistance to doxorubicin and paclitaxel in TNF-resistant cells. Additional evidence for the increased tumorigenesis found in our resistant cells can be found in studies reporting TNFR1 to be a tumor suppressor gene[48–50]. However, changes in TNFR1 expression have not been consistently correlated with decreased downstream TNF-induced cell death[9,51]. We demonstrate that decreased TNFR1 expression is associated with increased resistance to the cytotoxic effects of TNF. Yet, TNF signaling remains intact, as seen in the robust response of NF-κB activity in response to TNF administration in these cells. We hypothesize that the increased expression of TNFR2 may play a role in the enhanced TNF signaling in these cells. The TNFR2 receptor does not contain a death domain, which is responsible for recruitment of scaffolding proteins necessary for downstream apoptotic signaling[52]. However, TNRF2 can recruit TRAF2, which enables activation of the downstream NF-κB survival pathway[53]. Therefore, altered TNFR expression in these cells likely shifts TNF ligand binding from a cell death to pro-survival signal in these cells.

Downstream of TNFR, we identified altered signaling in the NF-κB survival pathway. We demonstrated increased protein levels of p50, as well as increased transcriptional activity of the p65 subunit, in our resistant cell model, which resulted in enhanced NF-κB mediated gene expression. Activation of NF-κB by TNFα is a strong anti-apoptotic signal that opposes apoptosis induced by TNFα[17,54]. NF-κB has been found to be constitutively activated in breast cancer compared to normal tissue and may be a key modulator of chemosensitivity[25]. Enhanced NF-κB signaling is thought to contribute to both endocrine resistance and chemoresistance in breast cancer[55]. Furthermore, studies have demonstrated that knocking down NF-κB can partially reverse resistance to both chemotherapy and endocrine therapy- induced apoptosis[56,57]. Therefore, it is likely that enhanced NF-κB signaling is at least partially responsible for the multi-drug resistance phenotype of these cells.

NF-κB not only promotes survival signaling, but is also intricately involved in the progression to an EMT phenotype, and subsequent metastasis in breast tumors[29]. We have identified several changes in both protein and mRNA expression indicative of EMT in our TNF-resistant breast cancer cells compared to parental cells. These include several genes known to be regulated by NF-κB. Our findings of decreased E-cadherin and increased vimentin expression are consistent with previously published studies involving overexpression of NF-κB[26]. We further identified various alterations in EMT genes, including Twist, and Slug. Our findings suggest that resistance to TNF confers an EMT phenotype to previously sensitive breast cancer cells. Several studies have demonstrated that EMT changes in breast tumors correlates with increased metastasis[58]. The development of drug resistance correlates with metastatic progression[59]. However, EMT changes alone are not sufficient to promote breast cancer metastasis, and the combination of EMT and increased NF-κB activity, as seen our MCF-7TN-R model, may be capable of inducing metastasis[29,60]. Taken together, our results demonstrate the specific protein and gene expression alterations involved in manipulating these pathways to promote chemoresistance.

Methods

Cell Culture. MCF-7 cells and MCF-7TN-R were cultured as previously described[61]. Briefly, the MCF-7 cell line used is a subclone of MCF-7 cells obtained from the American Type Culture Collection (Manassas, VA) generously provided by Louise Nutter (University of Minnesota, MN)[37]. MCF-7TN-R cells were generated by exposing MCF-7 cells to increasing concentration of TNFα until resistance was established[19]. The culture flasks were maintained in a tissue culture incubator in a humidified atmosphere of 5% CO_2 and 95% air at 37°C. For estrogen studies, cells

were washed with phosphate buffered saline (PBS) 3 times and grown in phenol red-free Dulbecco's Modified Eagle Medium (DMEM) supplemented with 5% dextran-coated charcoal-treated fetal bovine serum (5% CS-FBS) for 72 h before plating for each particular experiment.

Clonogenic Survival Assay. Colony assays were performed as described in previously published methods[62]. Cells were plated in 6-well plates at a density of 1000 cells per well in full DMEM media. Twenty-four hours later cells were treated with indicated concentrations of TNF and then monitored for colony growth. Ten days later the cells were fixed with 3% glutaraldehyde for 15 min. Following fixation, the plates were washed and stained with a 0.4% solution of crystal violet in 20% methanol for 30 min, washed with PBS, and dried. Colonies of ≥ 30 cells were counted as positive. Results were normalized to DMSO vehicle treated control cells.

Cell Viability Assay. Viability assays were performed as previously described[20,63]. Briefly, cells were plated at a density of 7.5×10^3 cells per well in a 96-well plate in phenol-red free DMEM supplemented with 5% FBS and allowed to attach overnight. Cells were then treated with the indicated drugs (ranging from 10 nM to 100 μM) for 24 h. Following treatment, 20 μL of 3-(4,5-Dimethylthiazol-2-yl)-2,5-diphenyltetrazolium bromide (MTT, 5 mg/ml) reagent was incubated in each well for 4 h. Cells were lysed with 20% SDS in 50% dimethylformamide. The pH and absorbances were read on an ELx808 Microtek plate reader (Bio-Tek Instruments, Winooski, VT) at 550 nm, with a reference wavelength of 630 nm.

Animals. Xenograft models were performed similar to previously reported studies[64]. In brief, Nu/nu immune-compromised female ovariectomized mice (29-32 days old) were obtained from Charles River Laboratories (Wilmington, MA). The animals were allowed a period of adaptation in a sterile and pathogen-free environment with sterile food and water *ad libitum*. Placebo or estradiol pellets (0.72 mg, 60-day release; Innovative Research of America, Sarasota, FL) were implanted s.c. in the lateral area of the neck in the middle point between the ear and shoulder using a precision trochar (10 gauge). MCF-7 or MCF-7TN-R cells in the exponential phase of growth were harvested using PBS/EDTA solution and washed. Viable cells (5×10^6) in a 50 μL sterile PBS suspension were mixed with 100 μL of either Matrigel or growth factor reduced Matrigel (BD Biosciences, Bedford, MA). Cells were injected in the mammary fat pad through a 5 mm incision in the hypogastric region, and the incision was closed using wound staples. All the procedures in animals were performed under anesthesia using a mix of isofluorane and oxygen delivered by mask. Tumor size was measured every 2 days using a digital caliper. The volume of the tumor was calculated using the following formula: $4/3\pi\ LS^2$ (L = larger radius; S = shorter radius). At necropsy on day 21, animals were euthanized by cervical dislocation after exposure to CO_2. Tumors were removed and either flash frozen in liquid nitrogen or fixed in 10% formalin for further analysis. All procedures involving these animals were conducted in compliance with State and Federal laws, standards of the U.S. Department of Health and Human Services, and guidelines established by the Tulane University Institutional Animal Care & Use Committee. This study was approved by the Tulane University Institutional Animal Care & Use Committee. The facilities and laboratory animal program of Tulane University- 3 -are accredited by the Association for the Assessment and Accreditation of Laboratory Animal Care.

Western Blot Analysis. Protein analysis was performed as described[61]. Briefly, cells were plated at 50–60% confluency in 10-cm² culture dishes in 5% DMEM for 48 h. Antibodies for Actin, TNFR1, TNFR2, p50, p65 and phospho-p65 were purchased from Cell Signaling Technology, Inc. (Beverly, MA). Membranes were incubated in primary antibody overnight at 4°C with gentle agitation. Secondary infrared conjugated antibodies were purchased from LI-Cor Biosciences (Lincoln, NE). Membranes were scanned using the LI-COR Odyssey imager and software (LI-COR Biosciences, Lincoln, Nebraska) to detect total and phosphorylated protein levels in cell lysates.

p65 NF-κB -Luciferase assay. As previously described, the cells were seeded in 24-well plates at a density of 5×10^5 cells/well in 10% DMEM media and allowed to attach overnight[65]. After 18 h, cells were transfected for 5 h in serum-free DMEM with 10 ng of pFC-NF-κB-luciferase plasmid, using 6 μl of Effectene (Qiagen) per μg of DNA. After 5 h the transfection medium was removed and replaced with phenol red-free DMEM supplemented with 5% CS-FBS containing vehicle or indicated concentration of TNF and incubated at 37°C. After 18 h the medium was removed, and 100 μl of lysis buffer was added per well and then incubated for 15 min at room temperature. Cell debris was pelleted by centrifugation at 15,000 x g for 5 min. Cell extracts were normalized for protein concentration using reagent according to the manufacturers protocol (BioRad Lab.). Luciferase activity for the cell extracts was determined using luciferase substrate (Promega Corp., Madison, WI) in an Autoluminat Plus luminometer (Berthhold Technologies, Bad Wildbad, Germany).

Real Time RT-PCR. Real time RT-PCR was performed similar to previously reported studies[66]. In brief, total cellular RNA was extracted using the RNeasy® mini column (Qiagen, Valencia, CA), following the manufacturer's instructions. Reverse transcription (RT) was performed using the SuperScript First-Strand Synthesis System for RT-PCR (Invitrogen). The level of gene transcripts was determined using the iQ5 real-time quantitative PCR detection system (BioRad Inc., Hercules, CA). Primer sequences are available in the Supplemental Methods Section. Quantification and relative gene expression were calculated with internal controls using the using

$2^{-\Delta\Delta Ct}$ method[67]. The ratio between these values obtained provided the relative gene expression levels.

Immunofluorescence analysis of EMT markers and morphology. Immunofluorescence was performed as previously described[68]. Briefly, the expression levels of an epithelial cell marker (E-cadherin) and a mesenchymal cell marker (vimentin) were assessed by indirect immunofluorescence using specific antibodies (E- cadherin: CS-3195 (Cell Signaling Technology, Beverly, MA, USA); vimentin: V6630 (Sigma, St. Louis, MO, USA). Cells were cultured in eight-well chamber slides for 48 h. The cells were fixed in 4% paraformaldhyde/PBS for 10 min followed by incubation with the primary antibodies and phalloidin at the desired dilution (E-cadherin: 1:50 dilution; vimentin: 1:50 dilution). Alexa 594 and 488 conjugated secondary antibodies (1:1,500 dilution) were used to detect E-cadherin and vimentin, respectively. The nucleus was stained using DAPI containing VectorShield mounting medium (Vector Laboratories, Burlingame, CA, USA). The digital images were captured using Nikon Eclipse 80*i* along with the accompanying program IPLab, version 3.6.5 (Nikon Inc., Melville, NY, USA).

Microarray data analysis and validation. Microarray analysis was performed according to previously published protocols[69]. The hybridized Human Genome U133A 2.0 Array was scanned and analyzed using the Affymetrix Microarray Analysis Suite version 5.0. The average density of hybridization signals from four independent samples was used for data analysis, and genes with signal density <300 pixels were omitted from the data analysis. P-values were calculated with two-sided t tests with unequal variance assumptions, and a P value of <0.001 was considered to be significant. The fold change was described as a positive value when the expression level was increased and a negative value when the expression level was reduced. False discovery rate was set at 0.1 in the data analysis. To confirm the gene expression data from microarray analysis, quantitative PCR was used to examine the mRNA levels of a subset of genes. The quantitative PCR results showed a high degree of correlation to the microarray data.

Statistical analysis. Statistical analysis of IC_{50} values were calculated from concentration-response curves using GraphPad Prism 5.0 (Graphpad Software, San Diego, CA), using the equation: Y = Bottom + (Top-bottom)/1 + 10LogEC50-X, assuming a standard slope, where the response goes from 10% to 90% of maximal as X increases over two log units. Differences in IC_{50} were compared using Student's unpaired t-test with p < 0.05 as the limit of statistical significance. Experiments comparing multiple concentrations to the control were tested with one-way ANOVA with Bonferroni post-test to compare individual concentrations. All statistical analyses were done using GraphPad Prism 5.0.

1. American Cancer Society. *v*. (The Society, Atlanta, GA, 2011).
2. Seidman, A. D. Chemotherapy for advanced breast cancer: a current perspective. *Seminars in oncology* **23**, 55–59 (1996).
3. Wang, G. H. *et al.* Bovine herpesvirus 4 BORFE2 protein inhibits Fas- and tumor necrosis factor receptor 1-induced apoptosis and contains death effector domains shared with other gamma-2 herpesviruses. *J Virol* **71**, 8928–8932 (1997).
4. Baker, S. J. & Reddy, E. P. Modulation of life and death by the TNF receptor superfamily. *Oncogene* **17**, 3261–3270 (1998).
5. Vandenabeele, P., Declercq, W., Beyaert, R. & Fiers, W. Two tumour necrosis factor receptors: structure and function. *Trends Cell Biol* **5**, 392–399 (1995).
6. Boldin, M. P. *et al.* Self-association of the "death domains" of the p55 tumor necrosis factor (TNF) receptor and Fas/APO1 prompts signaling for TNF and Fas/APO1 effects. *J Biol Chem* **270**, 387–391 (1995).
7. Hsu, H., Xiong, J. & Goeddel, D. V. The TNF receptor 1-associated protein TRADD signals cell death and NF-kappa B activation. *Cell* **81**, 495–504 (1995).
8. Peraldi, P., Hotamisligil, G. S., Buurman, W. A., White, M. F. & Spiegelman, B. M. Tumor necrosis factor (TNF)-alpha inhibits insulin signaling through stimulation of the p55 TNF receptor and activation of sphingomyelinase. *The Journal of biological chemistry* **271**, 13018–13022 (1996).
9. Zyad, A., Benard, J., Tursz, T., Clarke, R. & Chouaib, S. Resistance to TNF-alpha and adriamycin in the human breast cancer MCF-7 cell line: relationship to MDR1, MnSOD, and TNF gene expression. *Cancer Res* **54**, 825–831 (1994).
10. Herrnring, C. *et al.* Expression of the apoptosis-inducing ligands FasL and TRAIL in malignant and benign human breast tumors. *Histochem Cell Biol* **113**, 189–194 (2000).
11. Bebok, Z., Markus, B. & Nemeth, P. Prognostic relevance of transforming growth factor alpha (TGF-alpha) and tumor necrosis factor alpha (TNF-alpha) detected in breast cancer tissues by immunohistochemistry. *Breast Cancer Res Treat* **29**, 229–235 (1994).
12. Gaudet, M. M. *et al.* Genetic variation in tumor necrosis factor and lymphotoxin-alpha (TNF-LTA) and breast cancer risk. *Human genetics* **121**, 483–490 (2007).
13. de Jong, S., Timmer, T., Heijenbrok, F. J. & de Vries, E. G. Death receptor ligands, in particular TRAIL, to overcome drug resistance. *Cancer metastasis reviews* **20**, 51–56 (2001).
14. LeBlanc, H. *et al.* Tumor-cell resistance to death receptor--induced apoptosis through mutational inactivation of the proapoptotic Bcl-2 homolog Bax. *Nature medicine* **8**, 274–281 (2002).
15. Krajewski, S. *et al.* Prognostic significance of apoptosis regulators in breast cancer. *Endocr Relat Cancer* **6**, 29–40 (1999).

16. Buchholz, T. A. *et al.* Chemotherapy-induced apoptosis and Bcl-2 levels correlate with breast cancer response to chemotherapy. *Cancer J* **9**, 33–41 (2003).

17. Wang, C. Y., Mayo, M. W. & Baldwin, A. S., Jr. TNF- and cancer therapy-induced apoptosis: potentiation by inhibition of NF-kappaB. *Science* **274**, 784–787 (1996).

18. Nakshatri, H. & Goulet, R. J., Jr. NF-kappaB and breast cancer. *Curr Probl Cancer* **26**, 282–309 (2002).

19. Struckhoff, A. P. *et al.* Novel ceramide analogs as potential chemotherapeutic agents in breast cancer. *J Pharmacol Exp Ther* **309**, 523–532 (2004).

20. Antoon, J. W., White, M. D., Burow, M. E. & Beckman, B. S. Dual inhibition of sphingosine kinase isoforms ablates TNF-induced drug resistance. *Oncol Rep* **27**, 1779–1786 (2012).

21. Antoon, J. W. & Beckman, B. S. Sphingosine kinase: a promising cancer therapeutic target. *Cancer Biol Ther* **11**, 647–650 (2011).

22. Antoon, J. W. *et al.* Targeting NFkB mediated breast cancer chemoresistance through selective inhibition of sphingosine kinase-2. *Cancer Biol Ther* **11**, 678–689 (2011).

23. Chmura, S. J. *et al.* Loss of ceramide production confers resistance to radiation-induced apoptosis. *Cancer research* **57**, 1270–1275 (1997).

24. Lucci, A., Han, T. Y., Liu, Y. Y., Giuliano, A. E. & Cabot, M. C. Multidrug resistance modulators and doxorubicin synergize to elevate ceramide levels and elicit apoptosis in drug-resistant cancer cells. *Cancer* **86**, 300–311 (1999).

25. Weldon, C. B. *et al.* Sensitization of apoptotically-resistant breast carcinoma cells to TNF and TRAIL by inhibition of p38 mitogen-activated protein kinase signaling. *Int J Oncol* **24**, 1473–1480 (2004).

26. Chua, H. L. *et al.* NF-kappaB represses E-cadherin expression and enhances epithelial to mesenchymal transition of mammary epithelial cells: potential involvement of ZEB-1 and ZEB-2. *Oncogene* **26**, 711–724 (2007).

27. Hayden, M. S. & Ghosh, S. Signaling to NF-kappaB. *Genes & development* **18**, 2195–2224 (2004).

28. Cao, Y. & Karin, M. NF-kappaB in mammary gland development and breast cancer. *J Mammary Gland Biol Neoplasia* **8**, 215–223 (2003).

29. Huber, M. A. *et al.* NF-kappaB is essential for epithelial-mesenchymal transition and metastasis in a model of breast cancer progression. *J Clin Invest* **114**, 569–581 (2004).

30. Kang, Y. & Massagué, J. Epithelial-mesenchymal transitions: twist in development and metastasis. *Cell* **118**, 277–279 (2004).

31. Nieto, M. A. The snail superfamily of zinc-finger transcription factors. *Nat Rev Mol Cell Biol* **3**, 155–166 (2002).

32. Moreno-Bueno, G. *et al.* Genetic profiling of epithelial cells expressing E-cadherin repressors reveals a distinct role for Snail, Slug, and E47 factors in epithelial-mesenchymal transition. *Cancer Res* **66**, 9543–9556 (2006).

33. Al Saleh, S., Sharaf, L. H. & Luqmani, Y. A. Signalling pathways involved in endocrine resistance in breast cancer and associations with epithelial to mesenchymal transition (Review). *Int J Oncol* **38**, 1197–1217 (2011).

34. Rubio, M. F. *et al.* TNF-alpha enhances estrogen-induced cell proliferation of estrogen-dependent breast tumor cells through a complex containing nuclear factor-kappa B. *Oncogene* **25**, 1367–1377 (2006).

35. Park, K. J., Krishnan, V., O'Malley, B. W., Yamamoto, Y. & Gaynor, R. B. Formation of an IKKalpha-dependent transcription complex is required for estrogen receptor-mediated gene activation. *Mol Cell* **18**, 71–82 (2005).

36. Kerbel, R. S. Impact of multicellular resistance on the survival of solid tumors, including micrometastases. *Invasion Metastasis* **14**, 50–60 (1994).

37. Burow, M. E. *et al.* Differences in susceptibility to tumor necrosis factor alpha-induced apoptosis among MCF-7 breast cancer cell variants. *Cancer Res* **58**, 4940–4946 (1998).

38. Meacham, W. D., Antoon, J. W., Burow, M. E., Struckhoff, A. P. & Beckman, B. S. Sphingolipids as determinants of apoptosis and chemoresistance in the MCF-7 cell model system. *Exp Biol Med (Maywood)* **234**, 1253–1263 (2009).

39. Lee, S. H. & Nam, H. S. TNF alpha-induced down-regulation of estrogen receptor alpha in MCF-7 breast cancer cells. *Molecules and cells* **26**, 285–290 (2008).

40. Ben-Porath, I. *et al.* An embryonic stem cell-like gene expression signature in poorly differentiated aggressive human tumors. *Nature genetics* **40**, 499–507 (2008).

41. Gionet, N., Jansson, D., Mader, S. & Pratt, M. A. NF-kappaB and estrogen receptor alpha interactions: Differential function in estrogen receptor-negative and -positive hormone-independent breast cancer cells. *Journal of cellular biochemistry* **107**, 448–459 (2009).

42. Qiu, J. *et al.* Toll-like receptor 9 agonist inhibits ERalpha-mediated transactivation by activating NF-kappaB in breast cancer cell lines. *Oncol Rep* **22**, 935–941 (2009).

43. Biswas, D. K., Cruz, A. P., Gansberger, E. & Pardee, A. B. Epidermal growth factor-induced nuclear factor kappa B activation: A major pathway of cell-cycle progression in estrogen-receptor negative breast cancer cells. *Proceedings of the National Academy of Sciences of the United States of America* **97**, 8542–8547 (2000).

44. Vesuna, F. *et al.* Twist contributes to hormone resistance in breast cancer by downregulating estrogen receptor-alpha. *Oncogene* (2011).

45. Kuroki, J. *et al.* Cell-permeable ceramide inhibits the growth of B lymphoma Raji cells lacking TNF-alpha-receptors by inducing G0/G1 arrest but not apoptosis: a new model for dissecting cell-cycle arrest and apoptosis. *Leukemia* **10**, 1950–1958 (1996).

46. Zyad, A., Branellec, D., Mahe, Y., Tursz, T. & Chouaib, S. The development of human tumor-cell resistance to TNF-alpha does not confer resistance to cytokine-induced cellular cytotoxic mechanisms. *Int J Cancer* **52**, 953–958 (1992).

47. Bratton, M. R. *et al.* GalphaO Potentiates Estrogen Receptor-alpha Activity Via the Erk Signaling Pathway. *J Endocrinol* **214**, 45–54 (2012).

48. Chang, F., Lacey, M. R., Bouljihad, M., Honer Zu Bentrup, K. & Fortgang, I. S. Tumor necrosis factor receptor 1 functions as a tumor suppressor. *American journal of physiology. Gastrointestinal and liver physiology* **302**, G195–206 (2012).

49. Sasi, S. P. *et al.* Breaking the 'harmony' of TNF-alpha signaling for cancer treatment. *Oncogene* (2011).

50. Charles, K. A. *et al.* The tumor-promoting actions of TNF-alpha involve TNFR1 and IL-17 in ovarian cancer in mice and humans. *J Clin Invest* **119**, 3011–3023 (2009).

51. Cai, Z. *et al.* Alteration of the sphingomyelin/ceramide pathway is associated with resistance of human breast carcinoma MCF7 cells to tumor necrosis factor-alpha-mediated cytotoxicity. *J Biol Chem* **272**, 6918–6926 (1997).

52. Grell, M. *et al.* Induction of cell death by tumour necrosis factor (TNF) receptor 2, CD40 and CD30: a role for TNF-R1 activation by endogenous membrane-anchored TNF. *Embo J* **18**, 3034–3043 (1999).

53. Rothe, M., Sarma, V., Dixit, V. M. & Goeddel, D. V. TRAF2-mediated activation of NF-kappa B by TNF receptor 2 and CD40. *Science* **269**, 1424–1427 (1995).

54. Van Antwerp, D. J., Martin, S. J., Kafri, T., Green, D. R. & Verma, I. M. Suppression of TNF-alpha-induced apoptosis by NF-kappaB. *Science* **274**, 787–789 (1996).

55. Nakshatri, H., Bhat-Nakshatri, P., Martin, D. A., Goulet, R. J., Jr. & Sledge, G. W., Jr. Constitutive activation of NF-kappaB during progression of breast cancer to hormone-independent growth. *Molecular and cellular biology* **17**, 3629–3639 (1997).

56. Uetsuka, H. *et al.* Inhibition of inducible NF-kappaB activity reduces chemoresistance to 5-fluorouracil in human stomach cancer cell line. *Exp Cell Res* **289**, 27–35 (2003).

57. Wang, C. Y., Cusack, J. C., Jr., Liu, R. & Baldwin, A. S., Jr. Control of inducible chemoresistance: enhanced anti-tumor therapy through increased apoptosis by inhibition of NF-kappaB. *Nature medicine* **5**, 412–417 (1999).

58. Xue, C., Plieth, D., Venkov, C., Xu, C. & Neilson, E. G. The gatekeeper effect of epithelial-mesenchymal transition regulates the frequency of breast cancer metastasis. *Cancer research* **63**, 3386–3394 (2003).

59. Kerbel, R. S., Kobayashi, H. & Graham, C. H. Intrinsic or acquired drug resistance and metastasis: are they linked phenotypes? *Journal of cellular biochemistry* **56**, 37–47 (1994).

60. Lou, Y. *et al.* Epithelial-mesenchymal transition (EMT) is not sufficient for spontaneous murine breast cancer metastasis. *Developmental dynamics : an official publication of the American Association of Anatomists* **237**, 2755–2768 (2008).

61. Antoon, J. W. *et al.* Targeting NF-κB mediated breast cancer chemoresistance through selective inhibition of sphingosine kinase-2. *Cancer biology & therapy* **11,** 678–689 (2011).

62. Antoon, J. W. *et al.* Design, synthesis, and biological activity of a family of novel ceramide analogues in chemoresistant breast cancer cells. *J Med Chem* **52**, 5748–5752 (2009).

63. Antoon, J. W. *et al.* Novel D: -erythro N-octanoyl sphingosine analogs as chemo- and endocrine-resistant breast cancer therapeutics. *Cancer Chemother Pharmacol* **65**, 1191–1195 (2010).

64. Salvo, V. A. *et al.* Antiestrogenic glyceollins suppress human breast and ovarian carcinoma tumorigenesis. *Clin Cancer Res* **12**, 7159–7164 (2006).

65. Boue, S. M. *et al.* Identification of the potent phytoestrogen glycinol in elicited soybean (Glycine max). *Endocrinology* **150**, 2446–2453 (2009).

66. Rhodes, L. V. *et al.* Adult human mesenchymal stem cells enhance breast tumorigenesis and promote hormone independence. *Breast Cancer Res Treat* **121**, 293–300 (2010).

67. Schmittgen, T. D. *et al.* Quantitative reverse transcription-polymerase chain reaction to study mRNA decay: comparison of endpoint and real-time methods. *Analytical biochemistry* **285**, 194–204 (2000).

68. Zhou, C. *et al.* Proteomic analysis of tumor necrosis factor-alpha resistant human breast cancer cells reveals a MEK5/Erk5-mediated epithelial-mesenchymal transition phenotype. *Breast cancer research : BCR* **10**, R105 (2008).

69. Fan, M. *et al.* Diverse gene expression and DNA methylation profiles correlate with differential adaptation of breast cancer cells to the antiestrogens tamoxifen and fulvestrant. *Cancer research* **66**, 11954–11966 (2006).

Acknowledgements

Authors contributions

JA performed experiments and drafted the manuscript. AS carried out the MTT and western blot assay. RL performed microarray pathway and clustering analyses. AN and LR performed qPCR experiments. SE and VS performed animal studies. BS performed

immunofluorescence studies. KN and NS performed microarray analysis. Both MB and BS participated in the design and coordination of the study and helped to draft the manuscript. All authors read and approved the final manuscript.

Additional information